Research on
Engineering
Structures & Materials
journal homepage: http://jresm.org

RESEARCH
GROUP

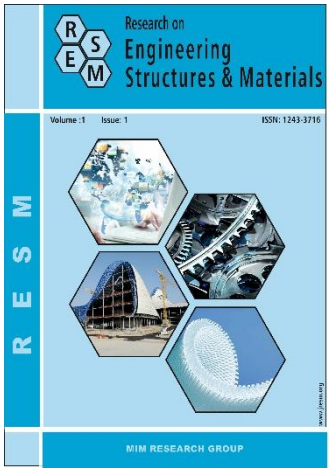

On the characterization of the free vibrations behavior of multiscale composite plates

Diogo Miguel Silva Costa, Maria Amélia Ramos Loja

Online Publication Date: 20 Aug 2017
URL: http://www.jresm.org/archive/resm2016.43st0602.html
DOI: http://dx.doi.org/10.17515/resm2016.43st0602

Journal Abbreviation: *Res. Eng. Struct. Mat.*

To cite this article
Costa DMS, Loja MAR. On the characterization of the free vibrations behavior of multiscale composite plates. *Res. Eng. Struct. Mat.*, 2017; 3(1): 27-44.

Research on
Engineering
Structures & Materials
journal homepage: http://jresm.org

RESEARCH GROUP

Research Article

On the characterization of the free vibrations behavior of multiscale composite plates

Diogo Miguel Silva Costa[1], Maria Amélia Ramos Loja[*1,2]

[1] GI-MOSM – Grupo de Investigação em Modelação e Optimização de Sistemas Multifuncionais, ISEL – Instituto Superior de Engenharia de Lisboa, Portugal
[2]LAETA, IDMEC – Instituto Superior Técnico – Universidade de Lisboa, Portugal

Article Info

Article history:
Received 2 Jun 2016
Revised 22 Jul 2016
Accepted 19 Aug 2016

Keywords:
Graded composites,
Hybrid multiscale particulate composites,
Carbon nanotube,
Free vibrations,
Parametric studies

Abstract

Multiscale functionally graded materials are characterized by possessing a continuous varying distribution of the micro and nano inclusion reinforcement particles through the matrix material. This continuity guarantees a smooth transition of material properties through the spatial domain of the composite and provides a great suitability to achieve specified structural responses. From the manufacturing point of view as well as from the computational perspective, these materials can be thought as effectively having a continuous variation of their properties, or as being constituted by a stacking of different layers, each having constant properties although following the continuous trend variation profile. Due to this ability to tailor the material to be used, and thus to obtain different structural responses, it is important to characterize the relative influence of material and geometrical parameters. These influences are investigated through a detailed parametric study.

1. Introduction

Composite materials are well known for their advantageous characteristics in different technological and scientific domains. Its wide dissemination during the most recent decades is not only due to an intense research effort but also because of the recognition of these advantages. The achievement of enhanced performances and in some cases of the optimal ones is a goal that may be succeeded through the adequate selection of the constituent materials, beyond the geometrical design itself. Composite materials in its broad sense have the ability to contribute to this goal at multiscale levels.

There is a significant number of research works on composite materials, with a particular focus on its micro and macro mechanics aspects, ranging from the different materials interaction analysis to the structural performance assessment. Among these works, we can refer in a more global perspective, the reviews of Gibson [1], Singh and Chauhan [2] and Lau et al. [3], among others. In his review work, Gibson [1] [1] tried to identify the most relevant topics in multifunctional composite materials and structures. He considered mechanical properties, such as strength, stiffness, fracture toughness, and damping, but also other factors, namely, electrical and/or thermal conductivity, sensing and actuation, energy harvesting/storage, self-healing capability, electromagnetic interference shielding, recyclability and biodegradability. According to the conclusions of this review, the majority of these recent developments are associated with polymeric composite materials and corresponding advances in nanomaterials and nanostructures. The review also concludes

*Corresponding author: amelialoja@dem.isel.ipl.pt
DOI: http://dx.doi.org/10.17515/resm2016.43st0602 Res.
Eng. Struct. Mat. Vol. 3 Iss. 1 (2017) 27-44

with a discussion of recent applications of multifunctional materials and structures, such as morphing aircraft wings, structurally integrated electronic components, biomedical nanoparticles for dispensing drugs and diagnostics, and optically transparent impact absorbing structures. Another review paper is due to Singh and Chauhan [2], and it is focused on the analysis of the feasibility and viability of developing low cost, high performance hybrid aluminium matrix composites for automotive and aerospace applications. This study considers fabrication characteristics and the mechanical behaviour of this type of composites. These parameters appreciation take into account the distribution of the reinforcing particles in the matrix alloy and the porosity levels. The authors concluded that the density, hardness, tensile behaviour and fracture toughness of these metal matrix composites were comparable or superior to the ceramic reinforced composites. As a final review work, with different characteristics from the previous two, we refer the one carried out by Lau et al. [3], which made a critical review on recent research related to nanotube/polymer composites, discussing as well recently-adopted coiled nanotubes to enhance the interfacial bonding strength of nanocomposites and the growth of nanotubes from nanoclay substrates to form exfoliated nanotube/nanoclay polymer composites.

Concerning to the study of the mechanical performance of functionally graded structural elements, we can say that there are many published works, but a much less number incorporating carbon nanotubes, which we may essentially find in these more recent years. Among other works on these hybrid advanced composites, we may refer the one due to Heshmati et al. [4] [4] which studied the effects of carbon nanotube length, waviness, agglomeration and distribution on the vibration behaviour of functionally graded nanocomposite beams reinforced by single-walled carbon nanotubes. To this purpose, and to determine the effective elastic properties of wavy carbon nanotubes (CNT) they have used Monte-Carlo simulation method. For the prediction of the elastic properties of the nanocomposite, a two-scale micromechanical model was developed. The numerical solutions were obtained using the finite element method and the Timoshenko beam formulation. The authors concluded that the parameters studied have a significant influence on the vibrational behaviour of the functionally graded nanocomposite beams.

Other works in this context of the nanocomposites are due to Mareishi et al. [5], Rafiee et al. [6][6], He et al. [7] [7] and Kamarian et al. [8] among other researchers. Mareishi et al. [5][5], presented an analytical solution for the nonlinear free and forced vibration response of smart laminated nano-composite beams resting on nonlinear elastic foundation and under external harmonic excitation. They have studied the effects of the applied voltage, temperature change, beam geometry, the volume fraction and the distribution of the carbon nanotubes on the nonlinear natural. Another work focused on the characterization of the influence of the applied voltage, plate geometry, volume fraction of fibers and weight percentage of single-walled and multi-walled carbon nanotubes on the linear and nonlinear natural frequencies of piezoelectric nanotubes/fiber/polymer multiscale composite plate, was carried out by Rafiee et al. [6]. This study was based on first-order shear deformation theory and considered von Kármán geometrical nonlinearity. He et al. [7] [7]presented an analytical formulation combined with a fractional-order time derivative damping model in order to study the large amplitude free and forced vibration response of carbon nanotubes/fiber/polymer laminated multiscale composite beams. That study was based on the Euler–Bernoulli beam theory and von Kármán geometric nonlinearity. The bulk material properties of the multiscale nanocomposite were predicted using Halpin–Tsai equations and fiber micromechanics. More recently, Kamarian et al. [8] carried out a parametric study is carried out to investigate the influences of carbon nanotubes volume fraction and agglomeration, fiber volume fraction, geometrical parameters and laminate lay-up on the natural frequencies

of multiscale nanocomposite plates, with a polymeric matrix phase. The authors have also considered the stacking sequence optimization of these plates to maximize their fundamental frequency using the firefly algorithm.

A recent work devoted to the analysis of functionally graded plates, was carried out by Bernardo et al.[9][9]. They presented a study on the characterization of the mechanical behaviour of functionally graded plates, using a meshless approach and kriging-based finite element method. On their work they considered the influence of using a discrete stacking of layers to approximate the continuous variation, as well as using different distributions of the reinforcement particles through the plate thickness. Different sandwich configurations and the effect of diverse material and geometrical parameters in the static and free vibrations behaviour of plates are also studied. Also in the context of the functionally graded materials, particularly on a study focused on the static bending and free vibration behavior of functionally graded beams resting on Winkler foundation, Akbaş [10] used a Navier-type solution for simply-supported boundary conditions, and proposed exact formulas for the static deflections and the fundamental frequencies. He considered the material properties varying through the thickness according to power law distribution and Euler-Bernoulli and Timoshenko beam theories. García-Macías et al.[11] also presented results associated to static and dynamic numerical simulations of thin and moderately thick functionally graded skew plates with uniaxially aligned reinforcements. To this study, a shell element based on first order shear deformation theory was formulated in oblique coordinates. According to the authors, the four-noded skew element presents a good performance. Parametric studies were carried out to explain the influences of the skew angle and other plate geometrical characteristics as well as the carbon nanotubes volume fraction. The fibre orientation was also analysed. The effect of a sudden transverse dynamic load produces in quadrilateral plates made with functionally graded composites reinforced with carbon nanotubes, was studied by Zhang et al.[12][12]. These authors considered the use of the first order shear deformation theory and the element-free IMLS-Ritz method. The numerical time integration is performed using the Newmark-b method. Numerical simulations were carried out to assess the effect of carbon nanotubes volume fraction and distribution type. The plate characteristics such as side angles, area and aspect ratios were also analysed. Also a recent work presented by Lei et al.[13] is related to the buckling behaviour of functionally graded composite laminated plate reinforced with carbon nanotubes. The authors have used the first-order shear deformation theory, implemented through the meshless kp-Ritz method. Parametric studies were developed for various types of nanotubes distributions, volume fraction and other geometrical characteristics. The number of layers and lamination angles were also considered.

From the literature research carried out, one may conclude that comparatively, a minor visibility was given to the metal matrix composites, as we may conclude upon the comprehensive works due to Esawi et al.[14] and Neubauer et al.[15].

Considering thus the importance to analyse and characterize the response of structures made of these type of multiscale materials, in the present work, the authors proceed to the study of moderately thick plates made of hybrid functionally graded materials, where the continuous phase is a nanocomposite of aluminium and carbon nanotubes, and the micro inclusions, ceramic particles, are incorporated in a graded manner. Parametric studies are developed, to characterize the influence of diverse material and geometrical parameters on the natural frequencies of this type of plates. For each case study, a set of results is presented either in tabular or graphical form.

2. CNT-metal nanocomposite

The mechanical behaviour of these functionally graded plates may be enhanced to some extent, by considering the dispersion of nano-inclusions in the continuous phase. This will yield a type of material which is commonly known as a multiscale hierarchical composite. In the present work it is considered that the metallic matrix (aluminium) may incorporate single-walled or multi-walled carbon nanotubes (SWCNT, MWCNT) and the resulting nanocomposite properties will be estimated through Halpin-Tsai equations 1-4, [16]. Assuming a perfect CNT dispersion within the matrix, the nanocomposite can be considered to be an isotropic material, which enables to write for the Young's modulus:

$$E_{mCN} = \frac{E_m}{8}\left(5\left(\frac{1+2\beta_{dd}V_{CN}}{1-\beta_{dd}V_{CN}}\right)+3\left(\frac{1+2\left(\frac{l_{CN}}{d_{CN}}\right)\beta_{dl}V_{CN}}{1-\beta_{dl}V_{CN}}\right)\right) \tag{1}$$

with:

$$\beta_{dl} = \frac{\left(\frac{E_{CN}}{E_m}\right)-\left(\frac{d_{CN}}{4t_{CN}}\right)}{\left(\frac{E_{CN}}{E_m}\right)+\left(\frac{l_{CN}}{2t_{CN}}\right)} \quad ; \quad \beta_{dd} = \frac{\left(\frac{E_{CN}}{E_m}\right)-\left(\frac{d_{CN}}{4t_{CN}}\right)}{\left(\frac{E_{CN}}{E_m}\right)+\left(\frac{d_{CN}}{2t_{CN}}\right)} \tag{2}$$

where E_{CN}, V_{CN}, l_{CN}, d_{CN}, and t_{CN}, stand for the Young's modulus, volume fraction, length, outer diameter, and thickness of the carbon nanotubes, respectively. E_m denotes the metallic matrix Young's modulus. The volume fraction of the carbon nanotubes is expressed as a function of the weight fraction of the nanotubes, as in Rafiee et al.[17]:

$$V_{CN} = \frac{w_{CN}}{w_{CN}+\left(\frac{\rho_{CN}}{\rho_m}\right)-\left(\frac{\rho_{CN}}{\rho_m}\right)w_{CN}} \tag{3}$$

Here w_{CN} and ρ_{CN}, denote the CNT weight fraction and density, and ρ_m the metallic matrix density respectively. The Poisson's ratio as well as the density of the nanocomposite is calculated by using the Voigt rule of mixtures:

$$\begin{aligned} \nu_{mCN} &= \nu_{CN}.V_{CN} + \nu_m.(1-V_{CN}) \\ \rho_{mCN} &= \rho_{CN}.V_{CN} + \rho_m.(1-V_{CN}) \end{aligned} \tag{4}$$

Low values of CNT weight fraction/volume fraction are considered, as it is known that higher values will compromise the perfect dispersion of the CNTs in the matrix, and therefore the isotropic assumption used in this study, would no longer be acceptable. Having these properties estimated, in a further step of the material construction, this nanocomposite will serve as the continuous phase of the constitution of a functionally graded material, by incorporating in a graded manner, ceramic particles.

3. Functionally graded multiscale ceramic-nanocomposites

The inclusion of the ceramic particles in the nanocomposite will be considered to vary continuously through the thickness direction, according to the volume fraction exponent power law [18]:

$$V_f = \left(\frac{1}{2}+\frac{z}{h}\right)^p \tag{5}$$

where h and z stand respectively for the whole thickness and the thickness coordinate, which has its origin at the middle surface of the graded composite. The exponent p permits an adjustment on the fastness the particles are incorporated closer to the bottom or top surfaces of the composite. This ability to vary the phases' mixture in a continuous way, may result in a composite more able to respond to specific requirements. It has additionally significant advantages concerning the minimization of stresses concentrations and may act as a thermal barrier when using ceramics.

The volume fraction distribution law in equation 5, is more commonly referred to the volume percentage of particles dispersed in the matrix. In this work the FGMs possess a metallic matrix hybridized or not with CNTs and incorporating different ceramic materials. Figure 1 depicts this volume fraction evolution for a dual-phase graded particulate composite, as a function of the exponent p.

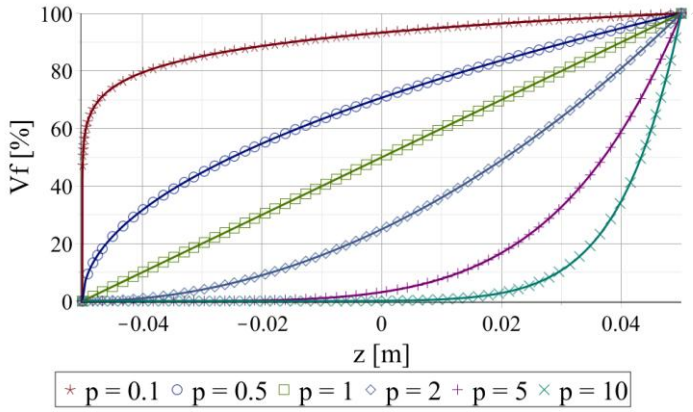

Fig. 1. Ceramic volume fraction distribution through FGM thickness without CNT

From this figure it results with clearness that the material average properties of the composite will also vary in a continuous form. The estimation of these macroscopic, average properties may be done through different homogenization schemes. In the cases presented in this work, we consider two schemes: Voigt rule of mixtures and Mori-Tanaka scheme. The validation study considers Mori-Tanaka homogenization scheme [19] for the estimation of the Young's modulus and Voigt rule for the Poisson's ratio and density of the nanocomposite. The remaining cases consider Voigt rule, which estimates the average material properties of the material, based only on the volume fraction of the different phases involved, as we can observe in equation 2 for a dual-phase composite (neglecting voids):

$$P_{ave} = P_m V_{fm} + P_c V_{fc} \quad ; \quad V_{fm} + V_{fc} = 1 \tag{6}$$

where P stands for a generic property. The subscripts *m,c* identify the metallic and ceramic phases and *ave* stands for the resulting material average property.

4. Finite Element Modelling

Considering the characteristics of the plate structures analysed in the present work, it was decided to use the first order shear deformation theory (FSDT) [20]. According to this theory, the displacements of an arbitrary point in the plate domain are given as:

$$\begin{aligned} u(x,y,z) &= u^0(x,y) + z.\theta_x^0(x,y) \\ v(x,y,z) &= v^0(x,y) + z.\theta_y^0(x,y) \\ w(x,y,z) &= w^0(x,y) \end{aligned} \tag{7}$$

where u^0, v^0 are the mid-plane membrane displacements and w^0 is the corresponding transverse displacement. θ_x^0 and θ_y^0 are respectively the rotations of the mid-plane about the x and y axes.

Considering the plate is made from a hybrid CNT-metal-ceramic composite, and assuming that this material may be regarded as an isotropic material, the state of strain is related to the state of stress through equations 8:

$$\begin{bmatrix}\sigma_x \\ \sigma_y \\ \sigma_{xy}\end{bmatrix} = \begin{bmatrix} Q_{11}(z) & Q_{12}(z) & 0 \\ Q_{12}(z) & Q_{22}(z) & 0 \\ 0 & 0 & Q_{66}(z)\end{bmatrix}.\begin{bmatrix}\varepsilon_x \\ \varepsilon_y \\ \gamma_{xy}\end{bmatrix}; \quad \begin{bmatrix}\sigma_{yz} \\ \sigma_{xz}\end{bmatrix} = \begin{bmatrix} k.Q_{44}(z) & 0 \\ 0 & k.Q_{55}(z)\end{bmatrix}.\begin{bmatrix}\gamma_{yz} \\ \gamma_{xz}\end{bmatrix} \tag{8}$$

The elastic coefficients Q_{ij} are widely described in the literature [20] for isotropic homogeneous materials. In this work, they may vary with the thickness coordinate. Concerning to the shear effects, and considering the theory that underlies this work, a shear correction factor (k) of 5/6, and a selective integration scheme were used. Following the usual procedure, one obtains the element matrices, which are given as:

$$K^e = \int_V B^T Q(z) B \, dV \quad ; \quad M^e = \int_V N^T \rho(z) N \, dV \tag{9}$$

where K^e and M^e are respectively the element stiffness and mass matrices. The matrix B expresses the relationship among the generalized strains and the generalized displacements, and N is the shape functions matrix. The density $\rho(z)$, as mentioned in a previous section is also a function of the thickness coordinate.

The equilibrium equation associated to a free vibration analysis, is compactly given as:

$$(\boldsymbol{K} - \boldsymbol{\omega_k^2 M})\boldsymbol{q_k} = \boldsymbol{0} \tag{10}$$

with $\boldsymbol{K}$ and $\boldsymbol{M}$ being respectively the global stiffness and mass matrices and $\boldsymbol{q}_k$ the generalized modal vector corresponding to a k-th natural frequency $\boldsymbol{\omega_k}$. The free vibrations analysis is carried out after the imposition of the adequate set of boundary conditions.

5. Results and Discussions

5.1. Validation study

The validation of the Lagrange quadrilateral plate finite element models implemented was carried out through the comparison of the present results with other authors' alternative

solutions [21]. This comparison is made for the first eight natural frequencies of a simply supported, functionally graded square plate with a unit edge length (a=1m) and an aspect ratio a/h=5. The material properties are given in Table 1.

Table 1. Material properties of constituent phases.

Constituent phase	Material properties
Metallic matrix (Al)	$E_m = 70$ GPa, $\nu_m = 0.3$, $\rho_m = 2700 - 2702\ kg/m^3$
Ceramic particles (ZrO_2)	$E_c = 151 - 200$ GPa, $\nu_c = 0.3$, $\rho_c = 5700\ kg/m^3$

The plate was discretized in 18x18 quadrilateral finite elements from Lagrange family, with four (Q4) and nine (Q9) nodes. The average Young's modulus was estimated using Mori-Tanaka method and the Poisson's ratio and the density were estimated through Voigt rule of mixtures. The first eight natural frequencies, obtained for different values of exponent of the volume fraction distribution power law, are presented in Table 2 in a non-dimensional form. The multiplier used to obtain these non-dimensional frequencies was $\bar{\omega} = \omega h\sqrt{\rho_m/E_m}$.

Table 2. Non-dimensional natural frequencies $\bar{\omega}$. $AlZrO_2$ thick plate.

p		Frequency modes							
		1	2	3	4	5	6	7	8
	[21]	0.2469	0.4535	0.4535	0.5441	0.5441	0.6418	0.7881	0.9076
Ceram	Present	0.2465	0.4541	0.4541	0.5421	0.5421	0.6429	0.7825	0.9116
	(%)	(0.16)	(0.13)	(0.13)	(0.37)	(0.37)	(0.17)	(0.71)	(0.44)
	[21]	0.2152	0.4114	0.4114	0.4761	0.4761	0.5820	0.6914	0.8192
1	Present	0.2187	0.4114	0.4114	0.4821	0.4821	0.5815	0.6971	0.8216
	(%)	(1.63)	(0)	(0)	(1.26)	(1.26)	(0.09)	(0.82)	(0.29)
	[21]	0.2153	0.4034	0.4034	0.4720	0.4720	0.5709	0.6817	0.8056
2	Present	0.2198	0.4035	0.4035	0.4821	0.4821	0.5702	0.6949	0.8053
	(%)	(2.09)	(0.02)	(0.02)	(2.14)	(2.14)	(0.12)	(1.94)	(0.04)
	[21]	0.2194	0.3964	0.3964	0.4760	0.4760	0.5611	0.6832	0.7928
5	Present	0.2233	0.3967	0.3967	0.4866	0.4866	0.561	0.6988	0.7936
	(%)	(1.78)	(0.08)	(0.08)	(2.23)	(2.23)	(0.02)	(2.28)	(0.10)
	[21]	0.2122	0.3897	0.3897	0.4675	0.4675	0.5517	0.6772	0.7615
Metal	Present	0.2118	0.3902	0.3902	0.4658	0.4658	0.5524	0.6724	0.7833
	(%)	(0.19)	(0.13)	(0.13)	(0.36)	(0.36)	(0.13)	(0.71)	(2.86)

To enable an easier appreciation of the deviations between the present results and the alternative solutions, the percent deviations are also included in the table, within parentheses, and were calculated as $\left(\left(\omega_i^{ref} - \omega_i^{pre}\right)/\omega_i^{ref}\right) \times 100$, where ω_i denotes the ith frequency, ref denotes the reference solution and pre the present solution. These frequencies were obtained for ceramic-rich and for metal-rich materials as well as for other exponent values of the exponent p. From the results in Table 2, it is possible to conclude on the low percent deviations between the present results and the references solutions [21] and therefore on the good agreement between them, despite the low aspect

ratio. To mention also that both elements (Q4 and Q9) gave similar results with the discretization used, thus one just presents one table.

5.2. Case studies

With the present work it is intended to characterize the free vibrations response of an FGM plate, namely by analysing the influence of a set of material and geometrical parameters. To achieve this goal, a simply supported FGM plate, with the same unit edge length (a=1m) was considered in most of the case studies. The exception is the case devoted to identify the influence of boundary conditions. The average properties were determined using Voigt rule of mixtures, and it was also considered the possibility of first hybridizing the metallic matrix with carbon nanotubes with different weight fractions.

The material properties of the used constituent metallic and the ceramic phases are given in Table 3.

Table 3. Material properties of constituent phases.

Constituent phase	Material properties
Metallic matrix (Al)	$E_m = 70$ GPa, $\nu_m = 0.3$, $\rho_m = 2700\ kg/m^3$
Ceramic material 1 (ZrO_2)	$E_{c,1} = 200$ GPa, $\nu_{c,1} = 0.3$, $\rho_{c,1} = 5700\ kg/m^3$
Ceramic material 2 (Al_2O_3)	$E_{c,2} = 380$ GPa, $\nu_{c,2} = 0.3$, $\rho_{c,2} = 3800\ kg/m^3$

To simplify, we will refer to FGM1 when considering the mixture of the aluminium matrix with the zirconia, and to FGM2 when using the mixture of the aluminium matrix with alumina. The geometrical and material properties of the carbon nanotubes [17] used to hybridize the metallic matrix are presented in Table 4.

Table 4. Material and geometrical properties of CNTs.

CNT	E_{CN} (GPa)	ν_{CN}	l_{CN} (μm)	d_{CN} (nm)	t_{CN} (nm)	ρ_{CN} (kg/m^3)
SW	640	0.33	25	1.4	0.34	1350
MW	400	0.33	50	20	0.34	1350

5.2.1. Influence of continuous and discrete approach

The first study carried out is related to the possibility of considering a layered stacking scheme to approximate the continuous variation intrinsically associated to the FGM concept. To this goal we have analysed two different situations, one where the mixture composition varied continuously and the other where a different number of layers were used. In this last case, one has considered three different numbers of layers, namely five, ten and fifty

Figure 2 illustrates the results obtained as function of MWCNT weight fractions (w_{CN}) and power law exponent (p), for five and fifty layers. The plate finite element used was Q9. In a global appreciation, we may conclude that the evolution pattern of the fundamental frequency for different MWCNT weight fractions and for different values of the exponent p, is clearly influenced by the number of layers considered in the discrete approach. From this figure, it is also conclusive that in the range of weight fractions analysed, the fundamental frequency decreases with the increase of the weight fraction. It is important

to note that this behaviour is expected, considering the geometrical characteristics of the MWCNTs, namely its aspect ratio, as shown in [22] although in the scope of the linear static analysis.

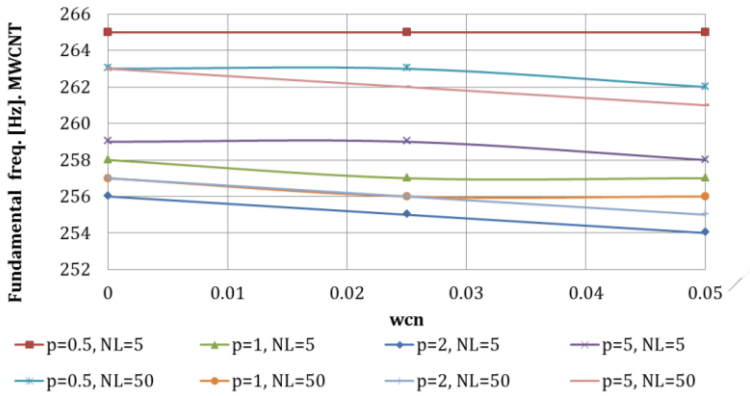

Fig. 2. Fundamental frequency ω vs MWCNT w_{CN}

It is also possible to understand that for exponent values lower or equal to one, a minor number of layers give higher values of frequency. When the exponent is higher than unity, a lower number of layers provide lower values of frequency. This illustrates the different ways, convergence to the continuous solutions occurs, as we may also see in Table 5 for the case w_{CN} =5%.

Table 5. Natural frequencies ω [Hz]. (a/h=20).

p		MWCNT, w_{CN} =5%				
		1	2	3	4	5
0.5	Cont.	262	648	648	1024	1270
	5	265	654	654	1033	1281
	10	263	650	650	1027	1274
	50	262	648	648	1024	1270
1	Cont.	256	631	631	998	1238
	5	257	634	634	1002	1242
	10	256	632	632	999	1239
	50	256	632	632	998	1238
2	Cont.	255	629	629	994	1232
	5	254	627	627	990	1228
	10	255	629	629	993	1231
	50	255	629	629	994	1232
5	Cont.	261	644	644	1016	1258
	5	258	636	636	1003	1243
	10	261	642	642	1013	1254
	50	261	644	644	1016	1258

Through Table 5 we can see that considering a number superior to ten layers already gives us good predictions when compared to the continuous solutions.

Table 6. Deviations (%) from continuous approach (a/h=20).

p		MWCNT, w_{CN} =5%				
		1	2	3	4	5
0.5	5	1.15	0.93	0.93	0.88	0.87
	10	0.38	0.31	0.31	0.29	0.31
	50	0.00	0.00	0.00	0.00	0.00
1	5	0.39	0.48	0.48	0.40	0.32
	10	0.00	0.16	0.16	0.10	0.08
	50	0.00	0.16	0.16	0.00	0.00
2	5	-0.39	-0.32	-0.32	-0.40	-0.32
	10	0.00	0.00	0.00	-0.10	-0.08
	50	0.00	0.00	0.00	0.00	0.00
5	5	-1.15	-1.24	-1.24	-1.28	-1.19
	10	0.00	-0.31	-0.31	-0.30	-0.32
	50	0.00	0.00	0.00	0.00	0.00

Complementing the previous results, and concerning to the deviations, taking as reference the continuous solutions, it is possible to observe in Table 6, the convergence patterns, qualitatively identified in Figure 2 and jointly commented with Table 5. These deviations were calculated as $((\omega_i^N - \omega_i^C)/\omega_i^C) \times 100$, where ω_i denotes the ith frequency, N stands for the number of layers considered in the discrete approach and C for the continuous one.

5.2.2. Influence of plate's aspect ratio

The influence of the aspect ratio is now considered. This parameter can be used as a first selection indicator of the shear deformation theory to use. It may also give us a preliminary perception of expectable deformations, in connection with the boundary conditions to which the plate is submitted. Two aspect ratios were chosen, a/h=10 and a/h=20 and the material used was the FGM1 with a mixture continuous variation.

The predicted fundamental frequencies, considering the dispersion or not, of multi-walled carbon nanotubes can be observed in Table 7.

From Table 7, we see that as expected, maintaining all the other characteristics, thicker plates possess higher fundamental frequencies when compared to thinner plates. It is also possible to observe that for exponent values greater than unity, the increasing dispersion of MWCNTs, lowers, although slightly, the fundamental frequency.

Table 7. Fundamental frequency ω [Hz] (MWCNT).

p	w_{CN} =0%		w_{CN} =2.5%		w_{CN} =5%	
	a/h=10	a/h=20	a/h=10	a/h=20	a/h=10	a/h=20
0	546	280	546	280	546	280
0.5	515	264	514	264	514	263
1	503	258	502	257	501	257
2	502	258	500	257	498	256
5	512	264	511	263	510	262

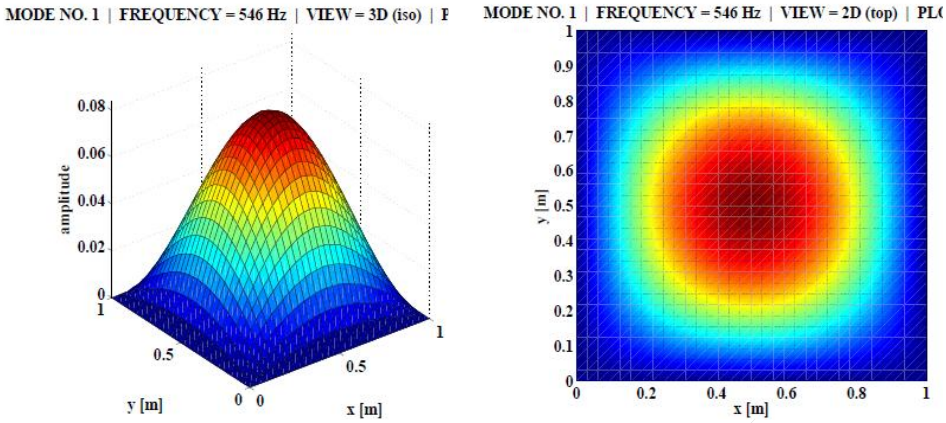

Fig. 3. Fundamental frequency ω (p=0)

Figure 3 depicts the fundamental vibration mode for a FGM1 plate with p=0. The evolution trend as a function of p, identified in previous cases, can also be verified here.

5.2.3. Influence of boundary conditions

To enable a conclusion on the influence of the boundary conditions of the plate, a set of cases was considered. The material and geometrical characteristics of the plate are the same as in the previous case study, considering additionally a SWCNT wcn=4%.

The characters C, S, F stand for clamped, simply supported and free respectively. As expected, stiffer boundaries yield higher frequencies and less stiff boundaries correspond to lower values of the natural frequencies. For illustrative purposes, Figure 4 presents two of the fundamental frequency mode shapes, corresponding to Table 8.

Table 8. Natural frequencies ω [Hz] (a/h=10, p=5).

BC	SWCNT, w_{CN} =4%				
	1	2	3	4	5
CFFF	102	238	595	622	757
SSSS	569	1351	1351	1830	1830
CCFF	613	710	1138	1554	1670
CCSF	641	950	1591	1725	1753
CCSS	792	1456	1748	1830	2322
CCCC	965	1830	1830	2556	3004

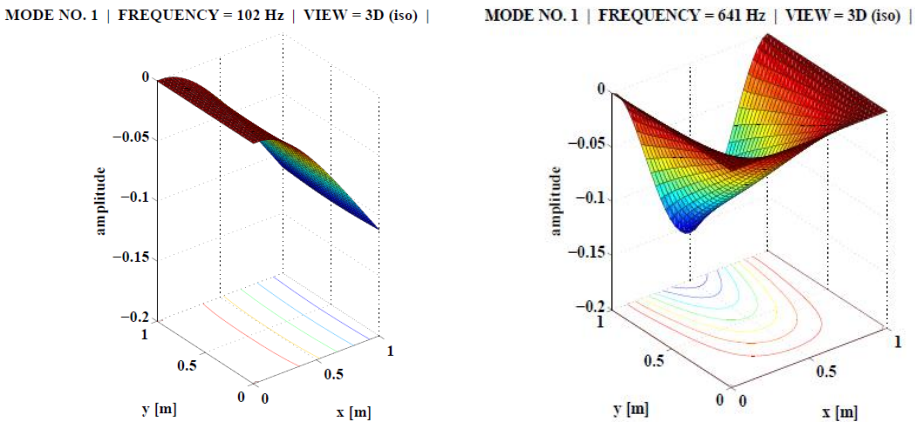

Fig. 4. Fundamental mode shapes. (left) CFFF, (right) CCSF boundary conditions

5.2.4. Influence of ceramic materials

Structures made of different materials with different elastic and mass characteristics will behave differently, namely considering its free vibration response. To illustrate this, we consider now both FGM1 and FGM2 and the hybridization of these materials with SWCNTs. An aspect ratio a/h=10 is chosen and the volume fractions continues to vary continuously. Similar meshes were used to this purpose. The fundamental frequencies obtained are presented in Table 9, for different values of the exponent p and CNTs weight fraction w_{CN}.

Table 9. Fundamental frequency ω [Hz].

p	FGM1			FGM2		
	w_{CN}=0%	w_{CN}=2.5%	w_{CN}=5%	w_{CN}=0%	w_{CN}=2.5%	w_{CN}=5%
0	546	546	546	921	921	921
0.5	515	528	541	784	798	812
1	503	525	545	707	732	756
2	502	533	560	642	680	714
5	512	550	584	606	651	692

In the present table, the fundamental frequencies allow concluding that the increase of SWCNTs weight fraction, produce higher values of frequencies no matter the FGM used. The other aspect that we can observe is that FGM2 due to its material properties yields higher values of fundamental frequencies.

It is also possible to understand from Table 9 and to see on Figure 5, that the fundamental frequency varies differently when CNTs are incorporated in the matrix. For the FGM2 a monotonic decreasing curve is always obtained.

This is not the case for the FGM1 case, which may be explained by the trade-off between the elastic and mass properties of the different constituents (See Table 6). This pattern was previously identified in another author's work [23].

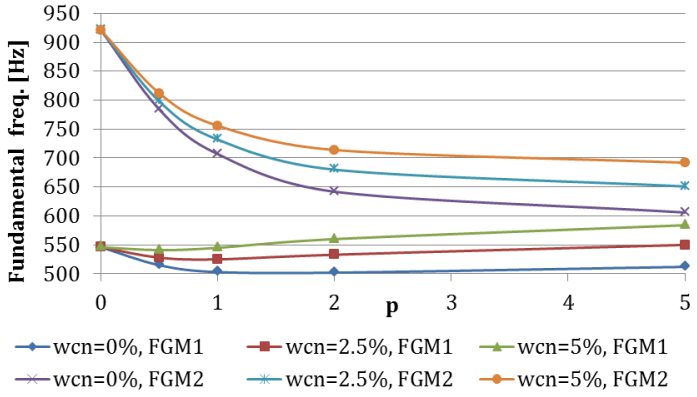

Fig. 5. Fundamental frequency ω (w/ SWCNT)

Table 10 presents the five first frequencies for functionally graded materials, FGM1 and FGM2, with and without single-walled carbon nanotubes.

Table 10. Natural frequencies ω [Hz].

Material	WCN (%)	Frequencies (SWCNT, p=5)				
		1	2	3	4	5
FGM1	0	263	647	647	1021	1265
	2.5	282	695	695	1096	1358
	5	300	738	738	1165	1443
FGM2	0	606	1449	1449	1991	1991
	2.5	651	1558	1558	2111	2111
	5	692	1654	1654	2226	2226

In both cases we observe that the frequencies increase with the inclusion on SWCNT, no matter the frequency mode considered.

5.2.5. Influence of carbon nanotubes

In this study we intend to illustrate the influence of the different types of CNTs. To that purpose, one has considered plates made of both FGMs and with an aspect ratio a/h=10, and assumed the volume fraction of the metal and ceramic to be varying in a continuous way.

The results for the different hybrid nanocomposites are firstly depicted in Figure 6 for an FGM1 plate. A first qualitative observation is related to the fact that SWCNTs provide a stiffening effect more visible when compared to the MWCNTS, being the fundamental frequencies higher in the first case.

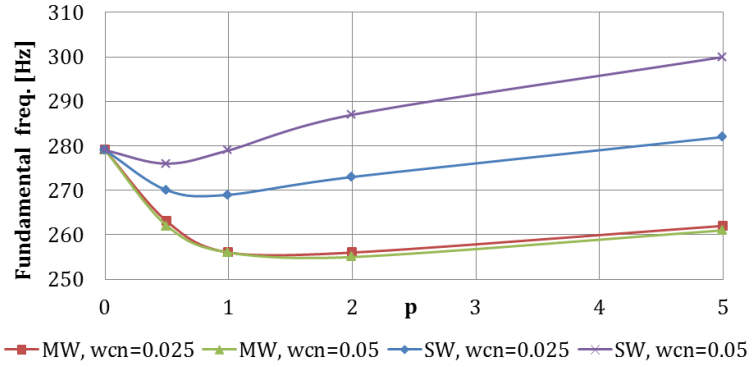

Fig. 6. Fundamental frequency vs exponent p. FGM1

To note a decreasing region associated to lower exponent values, as identified in previous cases. These observations, given for the cases where SWCNT were introduced, are complemented with the higher order frequencies evolution in Table 11.

Table 11. Natural frequencies ω [Hz]. FGM1 w/ SWCNT.

p	w_{CN} (%)	Frequencies modes				
		1	2	3	4	5
0	0	546	1312	1312	1839	1839
	2.5	546	1312	1312	1839	1839
	5	546	1312	1312	1839	1839
0.5	0	515	1240	1240	1784	1784
	2.5	528	1272	1272	1817	1817
	5	541	1301	1301	1848	1848
1	0	503	1212	1212	1748	1748
	2.5	525	1264	1264	1802	1802
	5	545	1311	1311	1855	1855
2	0	502	1205	1205	1701	1701
	2.5	533	1279	1279	1785	1785
	5	560	1345	1345	1864	1864
5	0	512	1224	1224	1639	1639
	2.5	550	1315	1315	1762	1762
	5	584	1398	1398	1878	1878

For illustrative purposes, in Figure 7 we can observe the second natural vibration mode for an FGM1 plate.

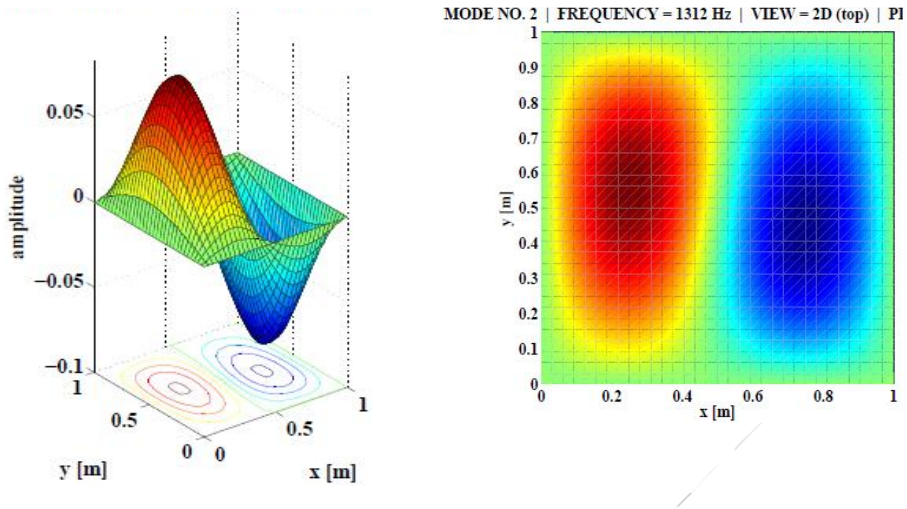

Fig. 7. Second vibration mode. FGM1, p=0

As we may conclude from the table, the frequencies increase with the SWCNT weight fraction, and the power law exponent. In Figures 8 and 9 we observe the fundamental frequency for FGM2 plates including increasing SWCNTs or MWCNTs weight fractions, respectively.

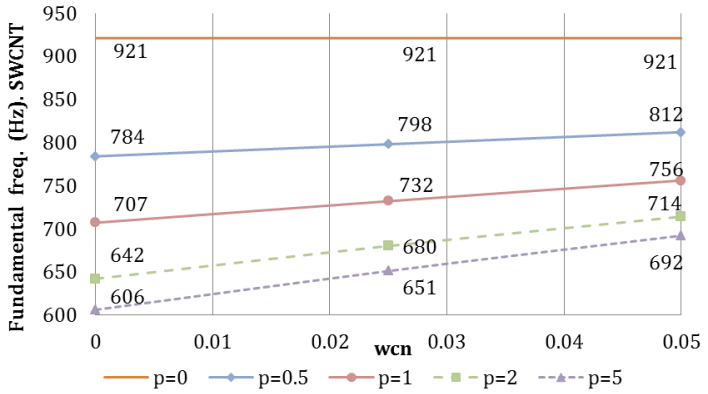

Fig. 8. Fundamental frequency vs w_{CN}. FGM2 with SWCNTs

When one considers the inclusion of SWCNTs, we can observe that for higher exponent values the increasing trends are higher, which is visible through the slope of those trends. To note also that in all the cases considered in Figure 8, the evolution is positive.

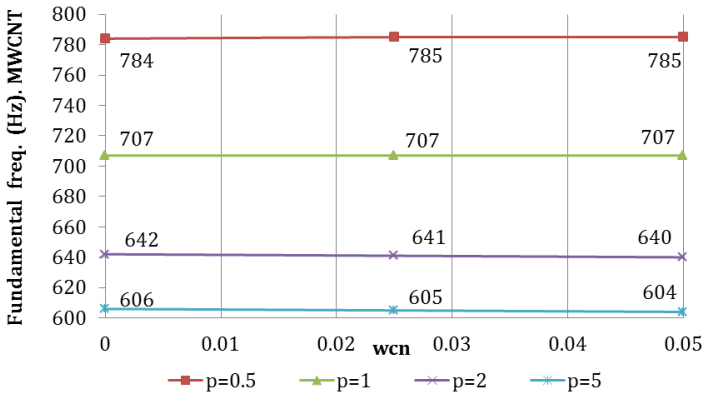

Fig. 9. Fundamental frequency vs w_{CN}. FGM2 with MWCNTs

The effect of the MWCNTs considered, follows a different trend as we can observe in Figure 9, particularly in the case of higher exponent values, where although small in the analysed range, a decreasing trend of the frequencies is observed when the weight fraction of the CNTs increases. This situation was already identified in a previous case study.

Table 12. Natural frequencies ω [Hz]. MWCNT.

p	WCN (%)	Frequencies modes				
		1	2	3	4	5
0	2.5	546	1312	1312	1839	1839
	5	546	1312	1312	1839	1839
0.5	2.5	514	1239	1239	1784	1784
	5	514	1237	1237	1784	1784
1	2.5	502	1208	1208	1747	1747
	5	501	1205	1205	1746	1746
2	2.5	500	1201	1201	1699	1699
	5	498	1197	1197	1698	1698
5	2.5	511	1221	1221	1635	1635
	5	510	1218	1218	1632	1632

This latter evidence is found also for the higher frequencies, as we can see in Table 12.

6. Conclusions

This work presents a study on the free vibrations response of moderately thick plates made of metal-ceramic functionally graded materials, where carbon nanotubes are dispersed in the metallic matrix. The parametric analyses carried out allowed characterizing the influence of material and geometrical properties of the plates analysed. Summarizing the results obtained in the different parametric studies carried out, it is possible to conclude that for the discretization used there is no significant difference between the two plate finite elements implemented. It is also possible to say that using a sufficiently large number of discrete layers with a constant volume fraction one converges to the results associated to the continuous volume fraction variation through thickness. Concerning to the dispersion of carbon nanotubes we conclude that single walled carbon nanotubes provide a clear stiffening effect visible in the higher frequencies values. These

patterns are verified for the weight fractions contents considered in this study. The inclusion of multi-walled carbon nanotubes present an inverse contribution, due to the specific characteristics of the nanotubes considered in the present study. The aspect ratio of the plates as well as its boundary conditions, are also relevant parameters. As we can conclude from the results obtained, thicker plates present higher frequencies and stiffer boundaries as well. When the plate includes the higher modulus ceramic it is also visible the expected response of higher frequencies values. Globally, one considers that the results obtained in this parametric study contributes to the better understanding of the free vibrations behaviour of metal-ceramic functionally graded materials with dispersed carbon nanotubes.

Acknowledgments

The authors acknowledge the support from Project LAETA, UID/EMS/50022/2013.

References

[1] Gibson RF. A review of recent research on mechanics of multifunctional composite materials and structures. Composite Structures, 2010; 2793:2810, 92.

[2] Singh J, Chauhan A. Characterization of hybrid aluminum matrix composites for advanced applications – A review. Journal of Materials Research and Technology, 2016: 159:169, 5(2).

[3] Lau K-T, Gu C, Hui D. A critical review on nanotube and nanotube/nanoclay related polymer composite materials. Composites: Part B 37, 2006; 425:436. http://dx.doi.org/10.1016/j.compositesb.2006.02.020

[4] Heshmat, M, Yas MH, Daneshmand F. A comprehensive study on the vibrational behavior of CNT-reinforced composite beams. Composite Structures, 2015; 434:448, 125.

[5] Mareish, S, Kalhori H, Rafiee M, Hossein, SM. Nonlinear forced vibration response of smart two-phase nano-composite beams to external harmonic excitations. Curved and Layered Structures, 2015; 2:150–161. http://dx.doi.org/10.1515/cls-2015-0008

[6] Rafiee M, Liu XF, He XQ, Kitipornchai S. Geometrically nonlinear free vibration of shear deformable piezoelectric carbon nanotube/fiber/polymer multiscale laminated composite plates. Journal of Sound and Vibration, 2014, 333, 3236–3251. http://dx.doi.org/10.1016/j.jsv.2014.02.033

[7] He XQ, Rafiee M, Mareishi S, Liew KM. Large amplitude vibration of fractionally damped viscoelastic CNTs/fiber/polymer multiscale composite beams. Composite Structures 2015, 131, 1111–1123. http://dx.doi.org/10.1016/j.compstruct.2015.06.038

[8] Kamarian S, Shakeri M, Yas MH. Natural Frequency Analysis and Optimal Design of CNT/Fiber/Polymer Hybrid Composites Plates Using Mori-Tanaka Approach, GDQ Technique, and Firefly Algorithm. Polymer Composites, 2016, 1-14. http://dx.doi.org/10.1002/pc.24083

[9] Bernardo GMS, Damásio FR, Silva TAN, Loja MAR. A study on the structural behaviour of FGM plates static and free vibrations analyses. Composite Structures, 2016; 124:138, 136.

[10] Akbaş ŞD. Free vibration and bending of functionally graded beams resting on elastic foundation. Research on Engineering Structures and Materials, 2015; 1: 25-37. http://dx.doi.org/10.17515/resm2015.03st0107

[11] García-Macías E, Castro-Triguero R, Flores EIS, Friswell MI, Gallego R. Static and free vibration analysis of functionally graded carbon nanotube reinforced skew plates. Composite Structures, 2016; 473:490, 140.
[12] Zhang LW, Xiao LN, Zou GL, Liew KM. Elastodynamic analysis of quadrilateral CNT-reinforced functionally graded composite plates using FSDT element-free method. Composite Structures, 2016; 144:154, 148.
[13] Lei ZX, Zhang LW, Liew KM. Buckling analysis of CNT reinforced functionally graded laminated composite plates. Composite Structures, 2016; 62:73, 152.
[14] Esawi AMK, Morsi K, Sayed A. Effect of carbon nanotube (CNT) content on the mechanical properties of CNT-reinforced aluminium composites. Composites Science and Technology 2010; 70: 2237–2241. http://dx.doi.org/10.1016/j.compscitech.2010.05.004
[15] Neubauer E, Kitzmantel M, Hulman M. Potential and challenges of metal-matrix-composites reinforced with carbon nanofibers and carbon nanotubes. Composites Science and Technology 2010; 70: 2228–2236. http://dx.doi.org/10.1016/j.compscitech.2010.09.003
[16] Halpin, JC, Kardos, JL. The Halpin-Tsai Equations: A Review. Polymer Engineering and Science, 1976; 344:352, 16(5).
[17] Rafiee M, He XQ, Mareishi S, Liew KM, Modeling and stress analysis of smart cnts/fiber/polymer multiscale composite plates. International Journal of Applied Mechanics, 2014; 1450025 (23 pages), 6(3).
[18] Ferreira AJM, Batra RC, Roque CMC, Qian LF, Martins PALS. Static analysis of functionally graded plates using third-order shear deformation theory and a meshless method. Composite Structures, 2005; 449:457, 69.
[19] Loja MAR, Barbosa JI, Mota Soares, CM. A Study on the Modeling of Sandwich Functionally Graded Particulate Composites. Composite Structures, 2012; 2209:2217, 94(7).
[20] Reddy JN, Mechanics of Laminated Composite Plates and Shells: Theory and Analysis, 2nd ed., CRC Press, 2004.
[21] Qian LF, Batra RC, Chen LM. Static and dynamic deformations of thick functionally graded elastic plates by using higher-order shear and normal deformable plate theory and meshless local Petrov–Galerkin method. Composites: Part B, 2004; 685:697, 35.
[22] Costa DMS, Loja MAR. Assessing the static behavior of hybrid CNT-metal-ceramic composite plates. AIMS Materials Science, 2016; 3(3): 808, 831.
[23] Loja MAR, Barbosa JI, Mota Soares CM. Analysis of Sandwich Beam Structures Using Kriging Based Higher Order Models. Composite Structures, 2015; 99:106, 119.